

A new algorithm for sky extraction for multi-fiber instrument

Rodrigues M.^{1,2}, Flores H.¹, Puech, M.¹, Yang Y³, and Royer. F¹

¹GEPI -Observatoire de Paris, 5 place Jules Janssen, 92190 Meudon, France

²CENTRA - Instituto Superior Tecnico, Av. Rovisco Pais, 1049-001 Lisboa, Portugal

³National Astronomical Observatories, 20A Datun Road, 100012 Beijing, PR China

July 1, 2021

Abstract

We present a new method to subtract sky light from faint object observations with fiber-fed spectrographs. The algorithm has been developed in the framework of the phase A of OPTIMOS-EVE, an optical-to-IR multi-object spectrograph for the future european extremely large telescope (E-ELT). The new technique overcomes the apparent limitation of fiber-fed instrument to recover with high accuracy the sky contribution. The algorithm is based on the reconstruction of the spatial fluctuations of the sky background (both continuum and emission) and allows us to subtract the sky background contribution in an FoV of $7 \times 7 \text{ arcmin}^2$ with an accuracy of 1% in the mono-fibers mode, and 0.3-0.4% for integral-field-unit observations.

1 INTRODUCTION

1.1 OPTIMOS-EVE

OPTIMOS-EVE (the Extreme Visual Explorer, PI: F. Hammer, GEPI and co-PI Lex Kaper, UvA) is a fibre-fed, optical-to-infrared multi-object spectrograph designed to explore the large field of view provided by the E-ELT at seeing limited conditions. It will enable to observe simultaneously multiple scientific targets in a $7'$ field of view with on of the three fiber setups provided, see figure 1. To achieve the scientific goals of OPTIMOS-EVE, the sky background has to be extracted with an accuracy $<1\%$.

1.2 Sky subtraction in fiber-fed instrument

Multi-fibre spectrographs are often suspected to suffer from a major drawback: the low accuracy of the sky subtraction process. Such a limitation is a critical

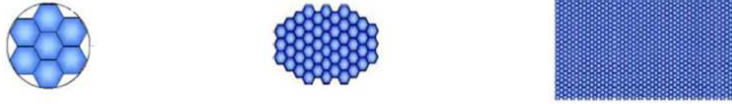


Figure 1: The three observational modes of OPTIMOS-EVE. From left to right: (1) the multi-object mode (MO). The MO LR mode will allow us to observe at low spectral resolution (LR, with $R=5000$) 240 objects with a total aperture on sky of $0.3''$. The medium and high resolution modes will allow us to observe 70 and 40 objects within a total aperture of $0.9''$ and $0.72''$ and a spectral resolution of 15 000 and 30 000, respectively; (2) the medium Integral Field Unit (MI): 30 IFUs composed of 56 fibers covering a surface of $2'' \times 3''$. The spatial sampling is $0.3''$ and the spectral resolution is $R=5000$; (3) Large integral field unit mode (LI). It is a large $15'' \times 9''$ IFU composed of 1650 fibers. The spectral and spatial resolutions are the same that in the MI mode.

issue for OPTIMOS-EVE, which aims to observe very faint objects. Contrary to slit spectroscopy that samples sky directly next to the object, the sky subtraction process in fiber spectroscopy is more problematic because the sky contribution cannot be sampled at the immediate vicinity of the target. This comparison has led to a commonly held view that accurate sky subtraction cannot be achieved with a multi-object fibre spectrograph. Several cons have been cited in literature against accurate sky subtraction with fiber-fed instruments, such as: spatial variations of the sky background, spatial variations of the quantum efficiency of the detector, variation of the fiber-to-fiber response (transmission, instrument flexure), scattered light, cross-talk between fibers [12], [11].

To overcome these difficulties, two standard observational procedures have been implemented to improve the efficiency of the sky subtraction process with fiber-fed instruments:

- **Simultaneous background:** Several fibers are dedicated to sample the sky contribution in the observed region. The number of sky fibers depends on the wavelength domain of the observations, the dimension of the field-of-view, and the requirement on the quality of the sky-subtraction [12]. Observations need to be previously corrected from the individual response of the fibers and scattered light.
- **Beam-switching:** Each fiber is alternatively switched between the object and a reference sky position (nodding). This strategy has the advantage of sampling the sky background with the same fibers that those used for observing the targets [11]. The sky and the science signals can be subtracted simultaneously. However, this procedure implies to dedicate half of the observation time for sky sampling and does not account for temporal variations of the sky background [8], [6].

However, even with these procedures the subsequent sky subtraction hardly reaches a quality better than 1%, i.e., a quality that can be easily reached with slit spectrographs. Therefore, we have designed a new method which take advantage of the spatial information provided by the multi-object mode and of

the prior knowledge on the nature of the sky, and in particular its spatial and temporal variations.

1.3 Sky variations

Knowing how the sky fluctuates in space and time is crucial for the implementation of an optimal sky subtraction. In this subsection we briefly describe the main characteristics of the sky variability.

The sky brightness ¹ show significant spatial and temporal variations [1],[9]. These are due to the dynamical nature of the atmosphere. Indeed, the atmosphere is a complex system in which the main properties at a given layer -composition, density, temperature - vary with time and space. The main factor of variation is the evolution of the chemical composition and density in the mesosphere, involved by harmonic periods of diurnal tides. Superposed to this smooth diurnal variations, the airglow emission is also affected by short-scale variations that are more problematic for spectroscopic observations. These short-period variations, of the order of few minutes to an hour, is due to perturbations in density and temperature within the upper atmosphere. Using FORS2 observations, we found that the sky background varies across the field ($5' \times 5'$) by 5-10%. The intensity of skylines also vary spatially from 10% to 20%. These spatial variations are smooth with a spatial scale of $1.0'$, which is coherent with the passage of gravity waves. In the near-IR ($1-1.8\mu m$), [8] and [7] have shown that the fluctuations of the OH emission bands can have variations of 5-10% and that the sky background fluctuates with an amplitude of 15% (see also [4]).

2 A new algorithm for sky extraction

The characterization of the spatial and temporal variations of the sky background allows us to optimize the algorithm of sky subtraction. As sky emission and sky continuum do not vary in phase, one can treat the two components independently. The algorithm is therefore divided into two steps: (1) the determination of the sky background using a $\lambda - \lambda$ surface reconstruction and (2) the extraction of the emission sky lines using the Davies' method [3]. A flowchart of the whole sky extraction algorithm is presented in Fig. 2

2.1 The sky continuum: $\lambda - \lambda$ reconstruction

The sky continuum is sampled at different spatial positions distributed over the instrument field of view using dedicated sky fibers. An interpolation method on an irregular grid is used to reconstruct a sky continuum surface over the total field of view, as a function of wavelength in regions free of emission sky lines. The three main steps are described below:

- (1) **Uncouple the continuum from the emission lines:** All sky spectra are stacked into a single sky spectrum in which a sigma-clipping algorithm is used to detect the emission sky lines. This step produces a sky emission

¹The skylight is made of a mixture of radiation produced by several sources such as moonlight, zodiacal light, airglow, thermal emission, unresolved background astrophysical sources, etc. In this work we have only taken into account the dominant source of sky in dark sites and optimal observational conditions: the emission of the upper atmosphere named airglow.

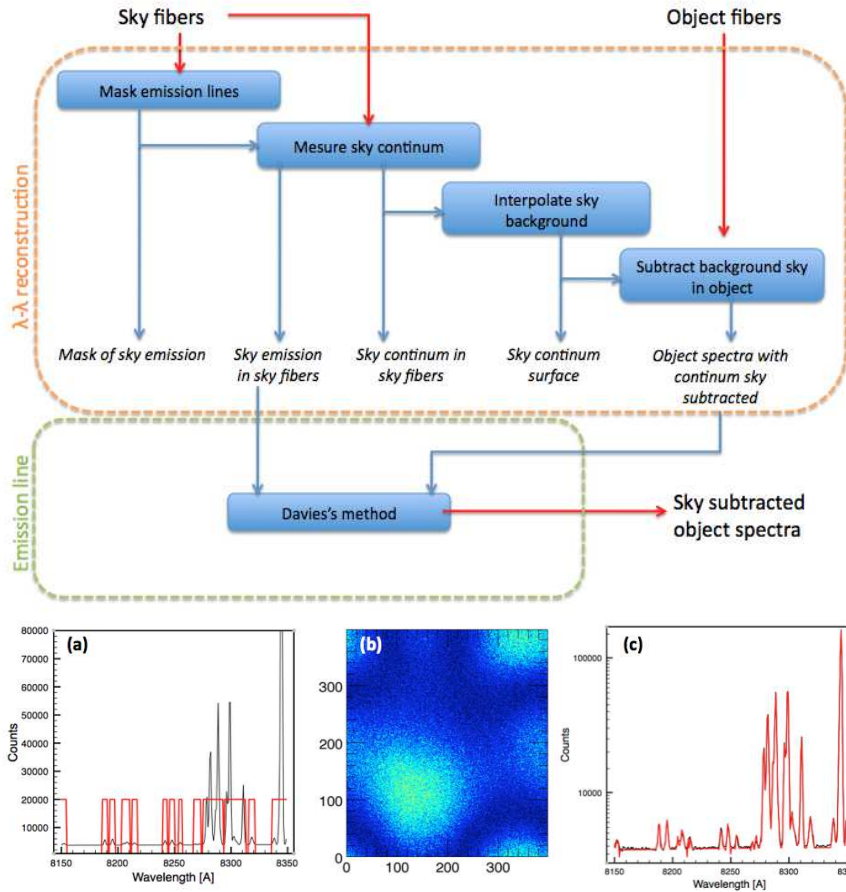


Figure 2: Flowchart of the sky subtraction algorithm. Examples are shown in the lower panels, with, from left to right: (a) sky emission mask (red boxes) produced by sigma-clipping, (b) residuals from the subtraction of the sky continuum over a $7' \times 7'$ field using 120 sky fibres and a 1h exposure time, (c) modeled sky background (red line) superimposed to the input sky spectrum (black line).

mask, which is used to mask all emission lines in the individual sky spectra and isolate spectral regions of pure continuum.

- (2) **Sky continuum extraction:** For each sky fibre, emission lines are masked with the sky emission mask derived from step (1). Regions without emission lines are filtered spectrally using a wavelet decomposition to improve their signal-to-noise ratio [10]. The smoothed continuum is then interpolated over the entire wavelength range in order to get a pure continuum sky spectrum in each sky fibre.
- (3) $\lambda - \lambda$ **surface reconstruction:** For each spectral element of resolution free of emission sky lines, a sky continuum surface is reconstructed thanks to a triangulation interpolation method, using the IDL routine GRID-DATA with a natural neighbor interpolation method.

At the end of this step, a $\lambda - \lambda$ sky continuum datacube is constructed, which summarizes all the constraints on the sky continuum over the field of view and wavelength bins. The sky continuum at the position of the sky and object fibres is extracted from this datacube, and subtracted to the sky and object individual spectra. Sky continuum subtracted spectra are then sent to the next step of the algorithm.

2.2 Removing emission sky lines

We used the method proposed by [3], which has been shown to be able to remove the OH lines in the near infrared (1 to 2.5 μm) with a good accuracy. This technique takes into account absolute and relative variations of OH sky line intensities, as well as variations due to instrumental flexures, which can impact the wavelength scale. The reader is referred to [3] for a detail description of the algorithm.

3 Sky subtraction with OPTIMOS-EVE

In order to test and optimize this algorithm for OPTIMOS-EVE, we have constructed a simulator for MO and MI EVE observational modes (see Sect. 1.1). This simulator is composed of a sky generator, which creates artificial sky datacubes, an object generator, which creates artificial science spectra, and an interactive routine that allows us to place IFUs or fibers within the EVE field of view. The parameters of the simulation have been chosen to be as close as possible of the EVE observational setups, in terms of spectral resolution, spatial scale, lambda sampling, and field-of-view. The architecture of the simulator is described on the flowchart shown in Fig. 3.

3.1 Accuracy on the sky background extraction

We have tested whether the designed algorithm can reach the required accuracy of $< 1\%$ on sky extraction required for both MO and MI observational modes. Hereafter, the quality of the extraction is defined as the mean residual between the input and the recovered sky surface as a function of wavelength.

In the MO mode, the quality of the sky continuum surface reconstruction depends on the number of dedicated sky fibers and how they are distributed

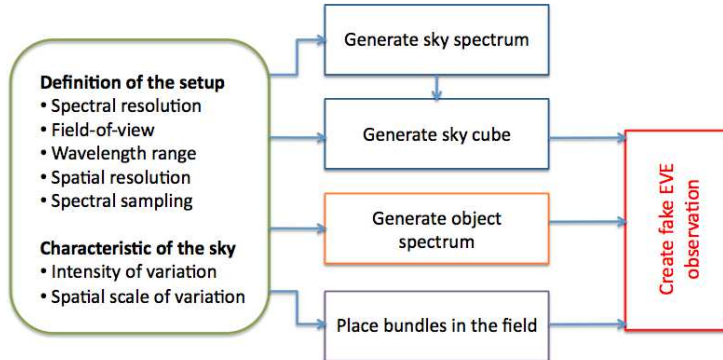


Figure 3: Flowchart of the simulator for the mono-fiber and IFU modes. The sky spectrum is generated from the combination of a sky continuum, given by the Standard ESO ETC sky brightness and [2], and a library of sky lines from [5]. The object spectrum is a high- z galaxy modeled by a constant continuum of magnitude mag_{con} and an emission line defined by a Gaussian shape centered at the position λ_{emi} with a total flux of $flux_{emi}$ and a velocity dispersion σ_{emi} .

over the field-of-view. We have first tested the quality of the sky continuum extraction as a function of the number of dedicated sky fibers. For a given number of sky fibers, we have simulated 50 observations of one hour exposure with sky fibers randomly distributed over the field of view, and measured the accuracy of the sky continuum extraction in a central $5' \times 5'$ region. Figure 4 illustrates the results of these Monte-Carlo simulations using the median value of the extraction quality over the 50 iterations which is plotted as a function of the number of sky fibers. At visible wavelengths, the sky continuum can be easily retrieved within a quality of 1% using 30-40 sky fibers. In the near IR, due to the more important variations of the sky background (20% peak to peak), at least 80 fibers are needed to properly recover the sky background with the same quality.

In the MI mode, we have simulated the case of an object illuminating nine central spaxels, which roughly corresponds to median seeing conditions. The remaining free fibers in the IFU were used as constraints for interpolating the sky background, in addition to four dedicated fibers sampling the sky contribution at larger spatial scales. The MI mode allows us to reach an accuracy on the sky extraction of 0.3%. It is thus recommended for observations for which the sky background has to be recovered with very high accuracy.

3.2 Application to observations of distant and faint galaxies

With OPTIMOS-EVE, it is required to observe very faint emission lines, down to $1 \times 10^{-19} \text{ ergs/cm}^2/\text{s}$, from objects with a continuum reaching $m_J = 28$ or more. We have verified the feasibility of this science case in term of sky subtraction, in the MO and MI modes. We have modelled an emission line (such as the Lyman α line) falling in a spectral window devoid of strong sky emission lines in the

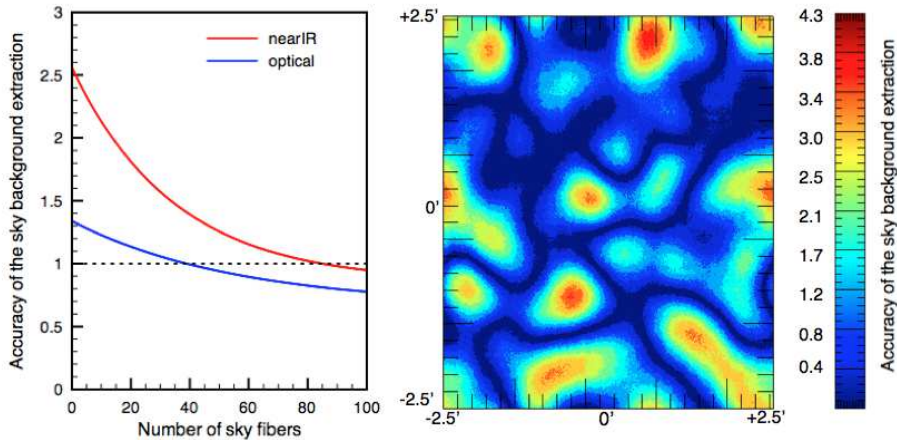


Figure 4: Right panel: Accuracy of the sky background subtraction as a function of the number of dedicated sky fibers for the optical (blue) and near IR (red) wavelength domain. Left panel: quality of the extracted sky background in the MO mode at visible wavelengths (%). Simulations were done on a field of 7×7 arcmin with 91 fibers randomly distributed on the sky. 110 objects fibers have been also distributed in the field of view. The quality of the sky background extraction in the object fibre is less than 0.9%.

J-band², i.e., ten magnitudes brighter than the object continuum. The test has been performed using a Monte-simulation of 40 independent observations of 1h exposure (40 different sky cubes) for each mode.

For the mode MO, 82 targets and 120 sky fibers have been distributed in the EVE field-of-view. Forty independent observations of 1h exposure have been generated using the EVE simulator. Each individual exposures have been sky-subtracted using the sky subtraction algorithm and then combined together with a median min-max rejection algorithm. Figure 6 summarizes the performance of the MO mode in recovering a distant galaxy with an AB magnitude of 28, an emission line flux of $1 \times 10^{-19} \text{ ergs/cm}^2/\text{s}$, and a $FWHM_{obs}=150\text{km/s}$, in 40 hr of integration time. The emission line is recovered with a mean S/N ratio of 8.

In MI mode, the galaxy illuminates nine spaxels of the IFU. The other spaxels of the IFU are used for the determination of the sky, in complement of the four surrounding sky fibers. As the MO mode, 40 independent observations of one hour exposure have been simulated. The sky has been extracted in each individual exposure, using an optimal extraction to subtract the sky contribution. The central IFU pixels have been stacked together, and then sky-subtracted. The MI mode allows us to reach an S/N of 5 and 16 for faint emission lines ($1 \times 10^{-19} \text{ ergs/cm}^2/\text{s}$) and an underlying continuum of 30 mag and 28 mag, respectively. Figure 6 shows the detected emission line after sky background subtraction (exposure time of 40 hours) in the MI and MO modes. In the MI mode, the sky background is better subtracted and the line is detected with a better S/N than with the MO mode.

²As a reference, the magnitude of the sky continuum in this band is 18.0 [?]000Msng.101....2C

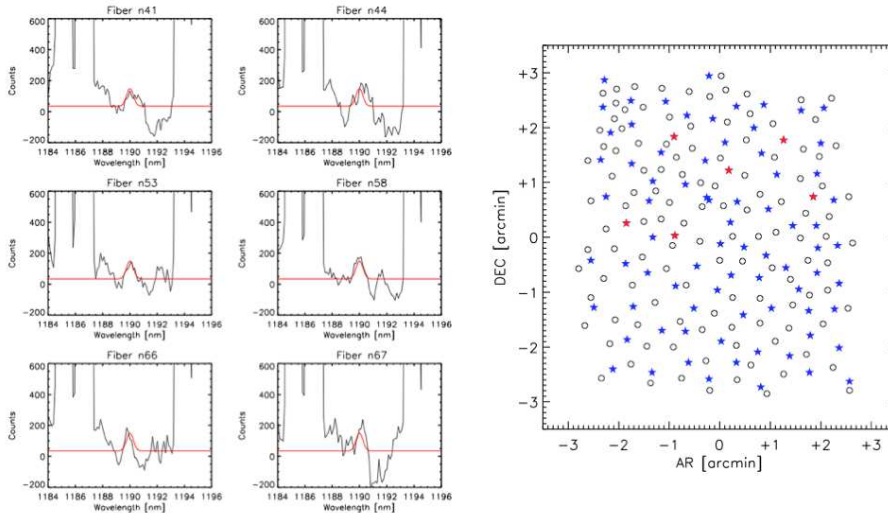


Figure 5: Simulation of 82 galaxies at $z=8.8$ in the J-band observed during 40 hours in the MO mode with ground-layer adaptive optics (GLAO). All galaxies have a continuum in the J-band of $m(AB)=28$ and the Lyman alpha line has an integrated flux of $1 \times 10^{-19} \text{ ergs/cm}^2/\text{s}$ and $\text{FWHM}=150\text{km/s}$. Left panels: the Lyman alpha line detected after sky background subtraction in different fibers (black line). The input spectrum is shown in red. The S/N of the detection depends on the quality of the sky background subtraction within each fiber. Emission sky lines have not been subtracted since such distant object emission lines are usually targeted in regions free of OH sky lines to boost the observational efficiency. Two sets of sky lines are visible at 1184-1187nm and 1193-1195nm. Right panel: EVE field-of-view and observational setup. The sky has been sampled with 120 fibers (half of the total number of available MO bundles; see open circles). The 82 simulated galaxies are shown as blue stars, while the red stars correspond to the fibers for which the measured spectra are shown in the left panels.

4 Conclusion

We have presented a new algorithm for sky subtraction dedicated to fibre-fed spectrographs, such as E-ELT/OPTIMOS-EVE. Spectroscopy of faint objects with fibre-fed instruments is often thought to be limited by the inability of such instruments to measure the sky contribution close enough to science targets. Using Monte-Carlo simulations, we have demonstrated that this new algorithm can nevertheless reach accuracies similar to slit spectrographs. This is due to a careful reconstruction of a sky continuum surface as a function of wavelength using dedicated sky fibres distributed over the whole instrument field-of-view. This makes it possible to interpolate the sky contribution at the location of the science channels with good accuracy. Objects as faint as $f_{Ly\alpha}=1 \times 10^{-19} \text{ ergs/cm}^2/\text{s}$ and $m_{cont} = 30$, which fairly represent $z=8.8$ Lyman-alpha emitters, should be detectable by the IFU mode of OPTIMOS-EVE within 40 hours of integration time.

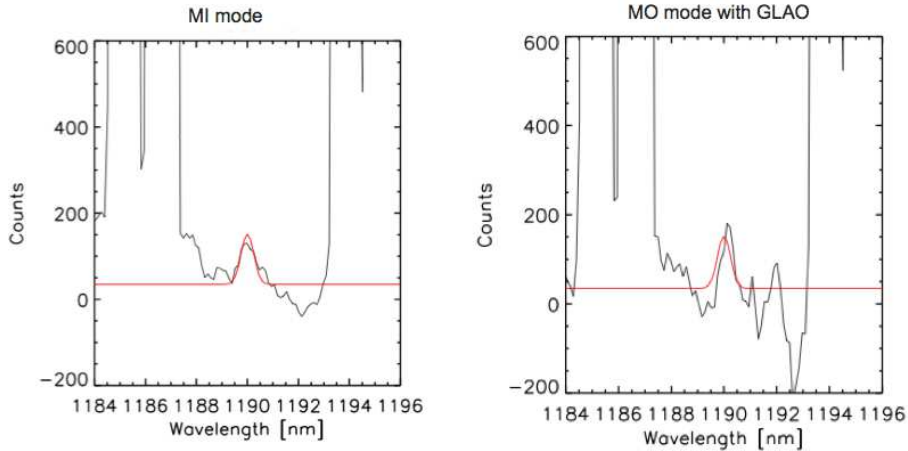


Figure 6: Simulation of a $z=8.8$ galaxy observed in the J band during 40 hours in the MI (left panels) and MO+GLAO (right panel) modes. The galaxy has a J-band continuum of $m(\text{AB})=28$ and the Lyman alpha line has an integrated flux of $1 \times 10^{-19} \text{ ergs/cm}^2/\text{s}$ with $\text{FWHM}=150\text{km/s}$. Left panel: the Lyman alpha line is detected in the stacked central IFU spaxels after sky background subtraction (black line). The target illuminates nine central spaxels that have been summed up. The remaining spaxels are used for sky sampling. Right panel: simulation of observations in the MO mode of the same Lyman alpha line. The observational setup is the same that the one described in Fig. .

References

- [1] J. W. Chamberlain. *Physics of the aurora and airglow*. International Geophysics Series, New York: Academic Press, 1961.
- [2] J. G. Cuby, C. Lidman, and C. Moutou. Isaac: 18 months of paranal science operations. *The Messenger*, 101:2–8, 2000.
- [3] R. I. Davies. A method to remove residual oh emission from near-infrared spectra. *MNRAS*, 375:1099–1105, 2007.
- [4] S. C. Ellis and J. Bland-Hawthorn. The case for oh suppression at near-infrared wavelengths. *MNRAS*, 386:47–64, 2008.
- [5] R. W. Hanuschik. A flux-calibrated, high-resolution atlas of optical sky emission from uves. *A&A*, 407:1157–1164, 2003.
- [6] G. Li Causi and M. de Luca. Optimal subtraction of oh airglow emission: A tool for infrared fiber spectroscopy. *New Astronomy*, 11:81–89, 2005.
- [7] G. Moreels, J. Clairemidi, M. Faivre, D. Pautet, F. Rubio da Costa, P. Rousselot, J. W. Meriwether, G. A. Lehmacher, E. Vidal, J. L. Chau, and G. Monnet. Near-infrared sky background fluctuations at mid- and low latitudes. *Experimental Astronomy*, 22:87–107, 2008.
- [8] S. K. Ramsay, C. M. Mountain, and T. R. Geballe. Non-thermal emission in the atmosphere above mauna kea. *MNRAS*, 259:751–760, 1992.

- [9] F. E. Roach and J. L. Gordon. *The light of the night sky*. Dordrecht, Boston, Reidel, 1973.
- [10] J.-L. Starck and F. Murtagh. Image restoration with noise suppression using the wavelet transform. *A&A*, 288:342–348, 1994.
- [11] F. Watson, A. R. Offer, I. J. Lewis, J. A. Bailey, and K. Glazebrook. Fiber sky subtraction revisited. In & Watson Arribas, Mediavilla, editor, *Fiber Optics in Astronomy III*, volume 152 of *Astronomical Society of the Pacific Conference Series*, pages 50–+, 1998.
- [12] R. F. G. Wyse and G. Gilmore. Sky subtraction with fibres. *MNRAS*, 257:1–10, 1992.